

# Variations of the Partial Short Range Order Structure of Amorphous $\text{Ni}_{32}\text{Pd}_{52}\text{P}_{16}$ During Relaxation Using Neutron Diffraction and Isotopic Substitution

M. Schaal, P. Lamparter, and S. Steeb

Max-Planck-Institut für Metallforschung, Institut für Werkstoffwissenschaften, Stuttgart

Z. Naturforsch. **43 a**, 1055–1060 (1988); received September 1988

Melt spun amorphous  $\text{Ni}_{32}\text{Pd}_{52}\text{P}_{16}$  specimens were produced using  $^{\text{nat}}\text{Ni}$ , the isotope  $^{60}\text{Ni}$ , and an isotopic mixture  $^{\text{e}}\text{Ni}$  with zero-scattering length. The specimens were heat treated for two hours at 496, 533, 570, and 607 K, respectively, and investigated by neutron diffraction. The Faber-Ziman structure factors as well as the total pair correlation functions show rather large effects caused by the relaxation procedure. By convenient combination of the total functions conclusions on the behaviour of the Ni–Ni, Ni–Pd, Ni–P, Pd–Ni, Pd–Pd, Pd–P, P–Ni, and P–Pd partial coordination numbers and atomic distances during the relaxation procedure are obtained. Relaxation has no detectable influence on the nearest neighbourhood but leads to variations in the region of the second Ni–Ni coordination sphere ( $3.7 \text{ \AA} \leq R \leq 5.7 \text{ \AA}$ ) with the main effect that after heat treatment at 607 K, 2 h, the second Ni–Ni coordination sphere is subdivided into three distinct subspheres. It is suggested that the relaxation process mainly involves the redistribution of bond angles.

## 1. Introduction

The relaxation of amorphous specimens during heat treatment was studied by diffraction methods for example with the Fe–B-, Co–B-, and Ni–B-systems [1], with  $\text{Fe}_{40}\text{Ni}_{40}\text{P}_{14}\text{B}_6$  [2], and with  $\text{Pd}_{82}\text{Si}_{18}$  [3]. Only small effects in the order of magnitude of maximum one percent of the structure factor could be observed. Since the thermal effects with amorphous Ni–Pd–P-alloys during relaxation are relatively large [4], we were able to observe variations of the pair correlation in amorphous  $\text{Ni}_{32}\text{Pd}_{52}\text{P}_{16}$  [5].

In order to treat not only the total pair correlation functions but as far as possible also partial functions we used neutron diffraction in the wide angle region together with isotopic substitution.

## 2. Experimental Procedure

In the present paper we use the total Faber-Ziman [6] structure factor  $S(Q)$ , which can be calculated from the corrected and normalized coherently scattered intensity  $I_{\text{coh}}(Q)$  and presented for a ternary system in terms of the six independent partial structure factors

$S_{ij}(Q)$  according to

$$\begin{aligned} S_{\text{tot}}(Q) &= \frac{I_{\text{coh}}(Q) - [\langle b^2 \rangle - \langle b \rangle^2]}{\langle b \rangle^2} \\ &= \frac{1}{\langle b \rangle^2} \sum_{i=1}^3 \sum_{j=1}^3 c_i c_j \cdot b_i b_j \cdot S_{ij}(Q) \\ &= \sum_{i=1}^3 \sum_{j=1}^3 W_{ij} S_{ij}(Q) \end{aligned} \quad (1)$$

with

$$\begin{aligned} \langle b \rangle &= c_1 b_1 + c_2 b_2 + c_3 b_3, \\ \langle b \rangle^2 &= c_1 b_1^2 + c_2 b_2^2 + c_3 b_3^2, \\ c_i &= \text{atomic fraction of component } i, \\ b_i &= \text{scattering length of component } i, \\ Q &= 4\pi(\sin \Theta)/\lambda, \\ 2\Theta &= \text{scattering angle}, \\ \lambda &= \text{wavelength}, \\ W_{ij} &= \frac{c_i c_j b_i b_j}{\langle b \rangle^2} = \text{weighting factor}. \end{aligned} \quad (1a)$$

For the determination of the six partial structure factors one needs six scattering experiments with different weighting factors. The variation of the  $W_{ij}$  can be achieved with neutron diffraction using isotopic substitution. In the present case of a  $\text{Ni}_{32}\text{Pd}_{52}\text{P}_{16}$ -alloy, however, only Ni-isotopes, especially  $^{60}\text{Ni}$  and  $^{62}\text{Ni}$  were available. Thus only the three specimens compiled in Table 1 with their weighting factors were used. For the calculation of the  $W_{ij}$  the scattering lengths from [7] were taken.

Reprint requests to S. Steeb, Max-Planck-Institut für Metallforschung, Institut für Werkstoffwissenschaften, Seestr. 92, D-7000 Stuttgart-1, FRG

0932-0784 / 88 / 1200-1055 \$ 01.30/0. – Please order a reprint rather than making your own copy.



Dieses Werk wurde im Jahr 2013 vom Verlag Zeitschrift für Naturforschung in Zusammenarbeit mit der Max-Planck-Gesellschaft zur Förderung der Wissenschaften e.V. digitalisiert und unter folgender Lizenz veröffentlicht: Creative Commons Namensnennung-Keine Bearbeitung 3.0 Deutschland Lizenz.

Zum 01.01.2015 ist eine Anpassung der Lizenzbedingungen (Entfall der Creative Commons Lizenzbedingung „Keine Bearbeitung“) beabsichtigt, um eine Nachnutzung auch im Rahmen zukünftiger wissenschaftlicher Nutzungsformen zu ermöglichen.

This work has been digitalized and published in 2013 by Verlag Zeitschrift für Naturforschung in cooperation with the Max Planck Society for the Advancement of Science under a Creative Commons Attribution-NoDerivs 3.0 Germany License.

On 01.01.2015 it is planned to change the License Conditions (the removal of the Creative Commons License condition “no derivative works”). This is to allow reuse in the area of future scientific usage.

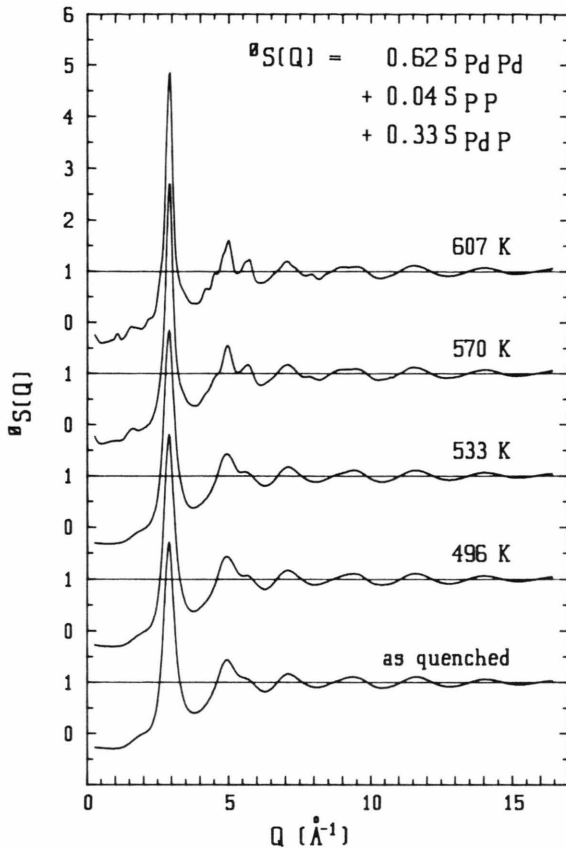


Fig. 1. Amorphous  $^{\phi}\text{Ni}_{32}\text{Pd}_{52}\text{P}_{16}$ ; neutron diffraction; total Faber-Ziman structure factor yielding  $0.62 S_{\text{PdPd}} + 0.33 S_{\text{PdP}} + 0.04 S_{\text{PP}}$ . Annealing time: 2 h.

Table 1. Faber-Ziman weighting factors according to (1 a).

Specimen	Structure factor	Faber-Ziman weighting factor					
		$W'_{\text{NiNi}}$	$W'_{\text{PdPd}}$	$W'_{\text{PP}}$	$W'_{\text{NiPd}}$	$W'_{\text{NiP}}$	$W'_{\text{PdP}}$
$^{\text{nat}}\text{Ni}_{32}\text{Pd}_{52}\text{P}_{16}$	$^{\text{nat}}S(Q)$	0.21	0.18	0.01	0.39	0.10	0.10
$^{60}\text{Ni}_{32}\text{Pd}_{52}\text{P}_{16}$	$^{60}S(Q)$	0.03	0.41	0.03	0.24	0.06	0.22
$^{\phi}\text{Ni}_{32}\text{Pd}_{52}\text{P}_{16}$	$^{\phi}S(Q)$	0.00	0.62	0.04	0.00	0.00	0.33

Table 2. Faber-Ziman weighting factors from linear combinations of measured total Faber-Ziman-structure factors.

Weighting of			Faber-Ziman weighting factors						Resulting distances	
$^{\text{nat}}S(Q)$	$^{60}S(Q)$	$^{\phi}S(Q)$	$W_{\text{NiNi}}$	$W_{\text{PdPd}}$	$W_{\text{PP}}$	$W_{\text{NiPd}}$	$W_{\text{NiP}}$	$W_{\text{PdP}}$		
0.00	0.00	1.00	0.00	0.62	0.04	0.00	0.00	0.33	Pd – Pd	Pd – P
−0.75	4.52	−2.76	0.00	0.00	0.00	0.79	0.21	0.00	Ni – Pd	Ni – P
6.55	−10.69	5.14	1.00	0.00	0.00	0.00	0.00	0.00	Ni – Ni	

$^{\text{nat}}\text{Ni}$  means nickel with natural isotopic abundance ( $b_{\text{natNi}} = 1.03 \cdot 10^{-12}$  cm),  $^{60}\text{Ni}$  means the isotope with  $b_{^{60}\text{Ni}} = 0.28 \cdot 10^{-12}$  cm, and  $^{\phi}\text{Ni}$  means a zero scattering mixture of 75.65 at.%  $^{60}\text{Ni}$  and 24.35 at.%  $^{62}\text{Ni}$ . The scattering lengths of Pd and P are  $0.591 \cdot 10^{-12}$  cm and  $0.513 \cdot 10^{-12}$  cm, respectively. Caused by the vanishing scattering length of  $^{\phi}\text{Ni}$  the weighting factors  $W'_{\text{NiNi}}$ ,  $W'_{\text{NiPd}}$ , and  $W'_{\text{NiP}}$  are zero in this case, and thus

$$^{\phi}S_{\text{tot}}(Q) = 0.62 S_{\text{PdPd}}(Q) + 0.04 S_{\text{PP}}(Q) + 0.33 S_{\text{PdP}}(Q). \quad (2)$$

The total structure factor obtained from the  $^{\phi}\text{Ni}_{32}\text{Pd}_{52}\text{P}_{16}$ -specimen thus yields direct information mainly on the Pd–Pd- and Pd–P-distributions. By convenient linear combinations of the three equations which can be established for the three specimens according to (1) and using the  $W'_{ij}$  from Table 1, further informations can be obtained.

During these linear combinations of equations attention must be paid to the fact that the resulting structure factor oscillates around unity at large  $Q$ 's. This is provided by multiplying each of the three measured structure factors  $^iS(Q)$  by a factor  $^iF$  with  $\sum_i ^iF = 1$ .

Table 2 shows the combinations most suitable for the evaluation of partial informations on the structure. These are those combinations where as many as possible coefficients vanish. With the third combination it became even possible to determine the partial structure factor  $S_{\text{NiNi}}(Q)$ .

Diffraction experiments were performed with the D4B-goniometer [8] at the high flux reactor of ILL, Grenoble, using neutrons with a wavelength of 0.7 Å. For the experimental details we refer to [9].

### 3. Results and Discussion

Figure 1 shows the total Faber-Ziman structure factors  $S(Q)$  as obtained with  $^{\phi}\text{Ni}_{32}\text{Pd}_{52}\text{P}_{16}$  in the

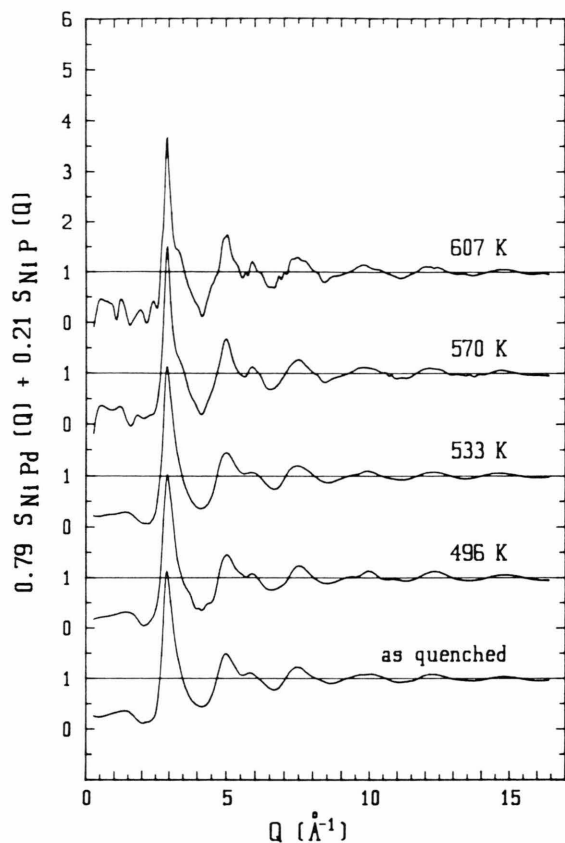


Fig. 2. Amorphous  $\text{Ni}_{32}\text{Pd}_{52}\text{P}_{16}$ ; neutron diffraction; combination of total structure factors according to second line in Table 2 yielding  $0.79 S_{\text{NiPd}} + 0.21 S_{\text{NiP}}$ . Annealing time: 2 h.

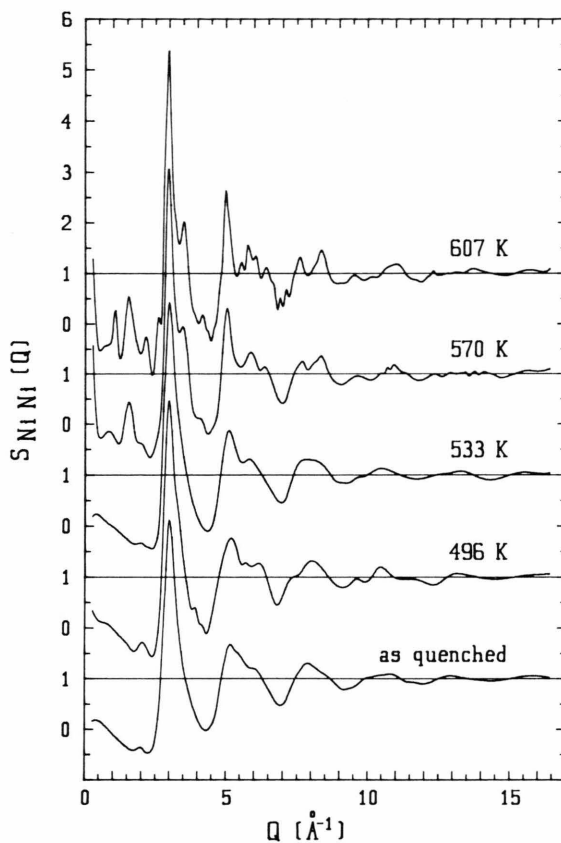


Fig. 3. Amorphous  $\text{Ni}_{32}\text{Pd}_{52}\text{P}_{16}$ ; neutron diffraction; combination of total structure factors according to third line in Table 2 yielding  $S_{\text{NiNi}}$ . Annealing time: 2 h.

as-quenched state and after annealing for 2 h at 496 K, 533 K, 570 K, and 607 K, respectively. The corresponding curves as obtained with  $^{\text{nat}}\text{Ni}_{32}\text{Pd}_{52}\text{P}_{16}$  and  $^{60}\text{Ni}_{32}\text{Pd}_{52}\text{P}_{16}$  are not reproduced here but can be found in [9]. Figure 1 shows that only the anneals at 570 K and 607 K caused a pronounced change of the structure factor compared to that obtained with the as-quenched specimen [5]. In Figs. 2 and 3 we present the combinations yielding  $0.79 S_{\text{NiPd}} + 0.21 S_{\text{NiP}}$  and  $S_{\text{NiNi}}$ , respectively.

The pair correlation functions  $G(R)$  as obtained from the structure factors of Figs. 1–3 by Fourier inversion are compiled in Fig. 4 in the  $R$ -region  $1.8 \text{ \AA} \leq R \leq 6 \text{ \AA}$ . The partial distances within the region of the first coordination sphere are very distinctively separated. This is not the case, however, for the P–P-distance because of the small weighting factor of the P–P correlation.

From the  $G(R)$ -curves the radial distribution functions  $\text{RDF}(R)$  are obtained:

$$\text{RDF}(R) = 4\pi R^2 \varrho_0 + R \cdot G(R) \quad (3)$$

$$= 4\pi R^2 \varrho_0 g(R) \quad (4)$$

with  $\varrho_0$  = mean atomic number density,  
 $\varrho(R) = \varrho_0 g(R)$  = local atomic number density.

Figures 5, 6, and 7 show the  $\text{RDF}(R)$ -functions as obtained from the  $G(R)$ -functions of Figure 4.

The identification of the peaks in the  $\text{RDF}(R)$ 's as individual pair correlations has been done from their positions in connection with the tabulated diameters of the atomic species and is marked in Figs. 5, 6, and 7. The partial coordination numbers were derived from Gaussian fitting to the peaks of the  $g(R)$ -functions

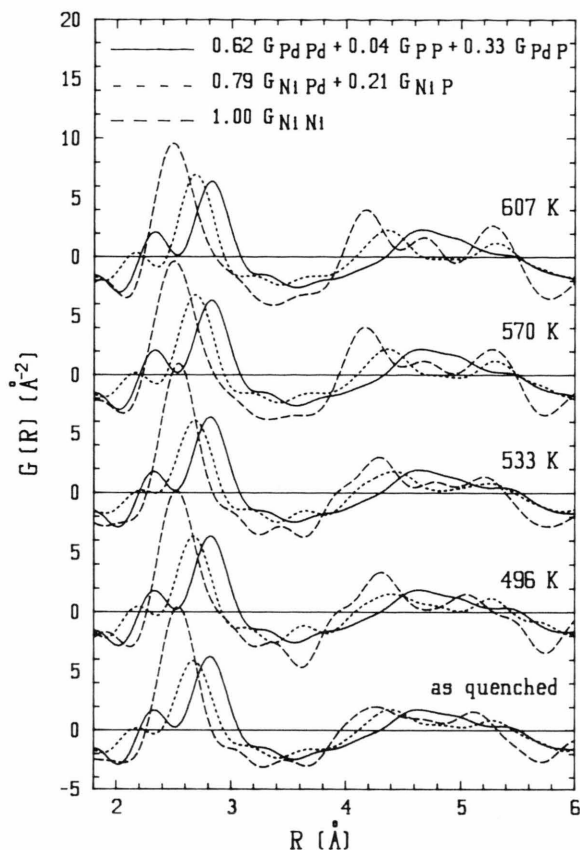


Fig. 4. Amorphous  $\text{Ni}_{32}\text{Pd}_{52}\text{P}_{16}$ ; neutron diffraction; pair correlation functions. Annealing time: 2 h.

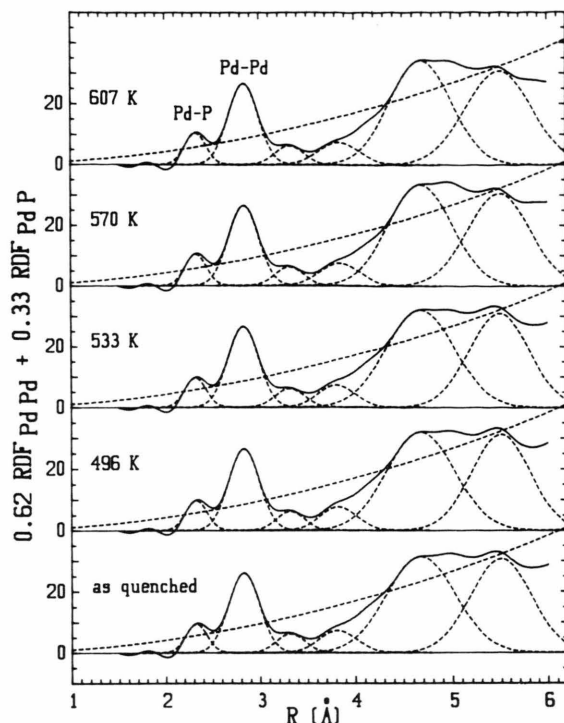


Fig. 5. Amorphous  $\text{Ni}_{32}\text{Pd}_{52}\text{P}_{16}$ ; radial distribution functions  $0.62 \text{ RDF}_{\text{PdPd}} + 0.33 \text{ RDF}_{\text{PdP}}$  according to Figure 1.  $\text{RDF}_{\text{PP}}$  in the ordinate is neglected because of the very small weighting factor.

Table 3. Amorphous  $\text{Ni}_{32}\text{Pd}_{52}\text{P}_{16}$ . Partial coordination numbers.

Heat treatment	Partial coordination numbers								
	Ni = central atom			Pd = central atom			P = central atom		
	$Z_{\text{NiNi}}$	$Z_{\text{NiPd}}$	$Z_{\text{NiP}}$	$Z_{\text{PdNi}}$	$Z_{\text{PdPd}}$	$Z_{\text{PdP}}$	$Z_{\text{PNi}}$	$Z_{\text{PPd}}$	$Z_{\text{PP}}$
as quenched	4.4	6.5	1.2	4.0	8.9	1.3	2.4	4.2	—
496 K, 2 h	4.1	6.4	1.3	3.9	9.0	1.4	2.6	4.4	—
533 K, 2 h	4.4	6.5	1.4	4.0	9.1	1.3	2.8	4.3	—
570 K, 2 h	4.2	6.8	1.2	4.2	8.9	1.4	2.4	4.7	—
607 K, 2 h	3.9	6.8	1.3	4.2	8.9	1.5	2.6	4.7	—

using fitting curves according to

$$f(R) = f_0 \exp \left[ -\frac{(R - R_0)^2}{2\sigma^2} \right] \quad (5)$$

with  $R_0$  = position of the symmetry centre of the Gaussian,

$\sigma$  = width of the Gaussian,

$f_0$  = maximum of the Gaussian.

These  $f(R)$ -functions were multiplied with  $4\pi R^2 \rho_0$  and then presented as broken lines in Figs. 5, 6, and 7. The partial coordination numbers then were obtained (see e.g. [10]):

$$Z_{ij} = \frac{c_j}{W_{ij}} 4\pi \rho_0 \int_0^\infty R^2 f(R) dR \quad (6)$$

with  $Z_{ij}$  = number of  $j$ -atoms around an  $i$ -atom.

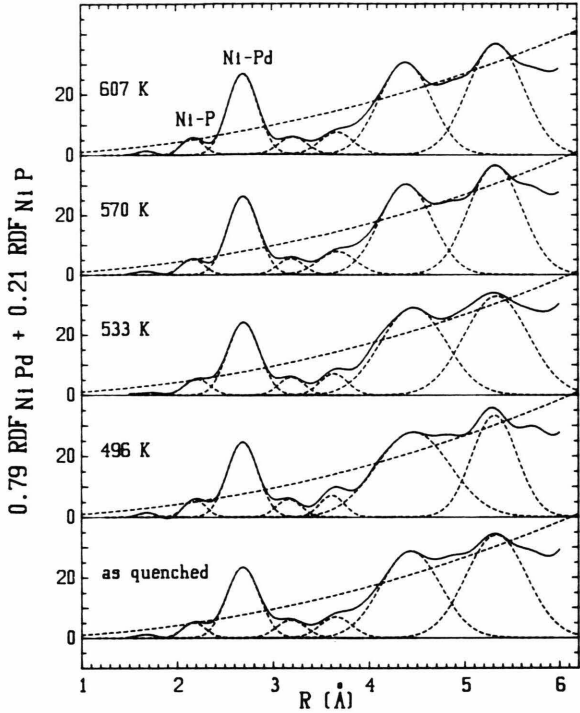


Fig. 6. Amorphous Ni<sub>32</sub>Pd<sub>52</sub>P<sub>16</sub>; radial distribution functions  $0.79 \text{RDF}_{\text{NiPd}} + 0.21 \text{RDF}_{\text{NiP}}$  according to Figure 2.

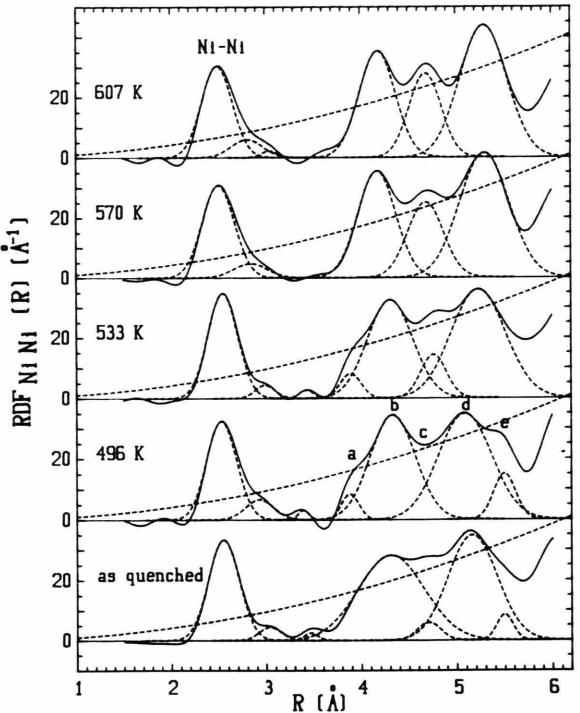


Fig. 7. Amorphous Ni<sub>32</sub>Pd<sub>52</sub>P<sub>16</sub>; partial radial distribution function  $\text{RDF}_{\text{NiNi}}$  according to Figure 3.

Table 4. Amorphous Ni<sub>32</sub>Pd<sub>52</sub>P<sub>16</sub>. Nearest neighbour distances and in brackets  $\sigma$  and  $f_0$  according to (5).

Heat treatment	Atomic distances [Å]				
	$R_{\text{NiP}}$	$R_{\text{PdP}}$	$R_{\text{NiNi}}$	$R_{\text{NiPd}}$	$R_{\text{PdPd}}$
as quenched	2.16 (0.12 1.03)	2.31 (0.11 1.64)	2.53 (0.16 4.58)	2.67 (0.17 3.06)	2.81 (0.16 3.07)
496 K, 2 h	2.18 (0.11 1.16)	2.32 (0.12 1.68)	2.51 (0.16 4.77)	2.67 (0.16 3.22)	2.81 (0.16 3.11)
533 K, 2 h	2.20 (0.14 1.02)	2.31 (0.12 1.67)	2.53 (0.16 5.04)	2.68 (0.16 3.13)	2.81 (0.16 3.12)
570 K, 2 h	2.16 (0.12 1.06)	2.32 (0.12 1.80)	2.49 (0.17 4.61)	2.68 (0.16 3.37)	2.82 (0.16 3.09)
607 K, 2 h	2.16 (0.12 1.13)	2.32 (0.12 1.81)	2.48 (0.16 4.60)	2.68 (0.16 3.43)	2.82 (0.16 3.12)

The resulting partial coordination numbers are compiled in Table 3, and the atomic distances as obtained from  $R_0$  according to (5) in Table 4.

Looking at the experimental results, i.e. the nearest neighbour distances and partial coordination numbers as presented in Tables 3 and 4, no changes in the atomic arrangement concerning the first coordination sphere during relaxation can be stated except perhaps a slight decrease of the Ni–Ni distance.

Apparently the rather strong changes of the structure factor during relaxation as observed in Figs. 1, 2, and 3 must be mainly due to changes in the higher coordination spheres [9]. The region of the second coordination sphere between 3.7 Å and 5.7 Å in Fig. 7 shows that relaxation first causes at 496 K the formation of shoulders a and e, whereas the small peak c vanishes. The main peak b increases while becoming narrower, and the other main peak d does not change.

At this temperature of 496 K the atomic arrangement apparently is most complex. During annealing at 533, 570, and 607 K the three maxima b, c, and d become more and more distinct, which leads to a clear subdivision of the second coordination sphere into three subspheres.

The distinct structural changes within the second coordination sphere during annealing, together with the nearly unchanged nearest neighbour correlations, gives evidence that the relaxation process is mainly associated with the redistribution of bond angles. The appearance and again the disappearance of features in the second sphere indicates that rather complex intermediate stages have to be passed through before the

relaxed state with three subspheres is reached. As bond angles are part of triplet correlations, it is not possible to extract more detailed information about them from the pair correlation functions derived in this work. For further progress comparison of three dimensional models with the present data will be essential.

#### Acknowledgements

Thanks are due to Deutsche Forschungsgemeinschaft, Bad Godesberg, for financial support and to Dr. P. Chieux, ILL, Grenoble, for his very intensive help during the experimental work.

- [1] W. Sperl, P. Lamparter, and S. Steeb, Report Nr. MPI/84/W1.
- [2] T. Egami, *J. Appl. Phys.* **50**, 1564 (1979).
- [3] E. Chason, K. F. Kelton, P. S. Pershan, L. Sorensen, F. Spaepen, and A. H. Weiss, in: S. Steeb and H. Warlimont (eds.), *Rapidly Quenched Metals (RQ 5)*, North Holland, Amsterdam 1985, pp. 683.
- [4] G. Schluckebier and B. Predel, *Z. Metallkunde* **74**, 569 (1983).
- [5] M. Schaal, P. Lamparter, and S. Steeb, proceedings of the 4th Int. Conference on non-crystalline materials (NCM4), Oxnard, USA from 18. 7. to 22. 7. 88 (1989).
- [6] T. E. Faber and J. M. Ziman, *Phil. Mag.* **11**, 153 (1965).
- [7] L. Koester and W. B. Yelon, *Neutron Diffraction Newsletter* (1983).
- [8] *Neutron Research Facilities at the ILL High Flux Reactor*, Edition 1986, Institut-Max von Laue-Paul Langevin, Grenoble, Frankreich 1986, p. 32.
- [9] M. Schaal, Doctor thesis, University Stuttgart 1988.
- [10] M. J. Huijben, Doctor thesis, University Groningen, Netherlands 1978.